ANTIOXIDANTS & REDOX SIGNALING
Volume 11, Number 9, 2009

DOI: 10.1089/ars.2009.2489

A Disruption in Iron-Sulfur Center Biogenesis *via* Inhibition of Mitochondrial Dithiol Glutaredoxin 2 May Contribute to Mitochondrial and Cellular Iron Dysregulation in Mammalian Glutathione-Depleted Dopaminergic Cells: Implications for Parkinson's Disease

Donna W. Lee, Deepinder Kaur, Shankar J. Chinta, Subramanian Rajagopalan, and Julie K. Andersen

Abstract

Parkinson's disease (PD) is characterized by early glutathione depletion in the substantia nigra (SN). Among its various functions in the cell, glutathione acts as a substrate for the mitochondrial enzyme glutaredoxin 2 (Grx2). Grx2 is involved in glutathionylation of protein cysteine sulfhydryl residues in the mitochondria. Although monothiol glutathione–dependent oxidoreductases (Grxs) have previously been demonstrated to be involved in iron-sulfur (Fe-S) center biogenesis, including that in yeast, here we report data suggesting the involvement of mitochondrial Grx2, a dithiol Grx, in iron-sulfur biogenesis in a mammalian dopaminergic cell line. Given that mitochondrial dysfunction and increased cellular iron levels are two important hallmarks of PD, this suggests a novel potential mechanism by which glutathione depletion may affect these processes in dopaminergic neurons. We report that depletion of glutathione as substrate results in a dose-dependent Grx2 inhibition and decreased iron incorporation into a mitochondrial complex I (CI) and aconitase (m-aconitase). Mitochondrial Grx2 inhibition through siRNA results in a corresponding decrease in CI and m-aconitase activities. It also results in significant increases in iron-regulatory protein (IRP) binding, likely as a consequence of conversion of Fe-S–containing cellular aconitase to its non–Fe-S–containing IRP1 form. This is accompanied by increased transferrin receptor, decreased ferritin, and subsequent increases in mitochondrial iron levels. This suggests that glutathione depletion may affect important pathologic cellular events associated with PD through its effects on Grx2 activity and mitochondrial Fe-S biogenesis. *Antioxid. Redox Signal.* 11, 2083–2094.

Introduction

PARKINSON'S DISEASE (PD) is an age-related progressive neurodegenerative disorder characterized by preferential loss of dopaminergic (DA) neurons in the substantia nigra (SN), a region of the midbrain involved in coordinating voluntary motor movement (6). Physiologically, PD is characterized by midbrain dopamine deficiency owing to the degeneration of these neurons (10). Its pathologic features also include the presence of intracytoplasmic inclusions known as Lewy bodies (18). Multiple lines of evidence implicate both oxidative stress and mitochondrial dysfunction in cell death associated with PD.

Glutathione plays multiple roles in the nervous system, both as an antioxidant and as a redox modulator. Depletion in levels of total glutathione (GSH + GSSG) is one of the earliest reported biochemical events reported to occur in the parkinsonian SN (2, 22, 36, 37). Previous studies from our laboratory demonstrated that total glutathione reduction within dopaminergic cells resulted in selective CI inhibition and subsequent mitochondrial dysfunction, which ultimately leads to cell death (11, 12, 22, 24), indicating that maintenance of thiol homeostasis may be critical for protecting midbrain dopaminergic neurons.

In addition to its several other known cellular functions, reduced glutathione (GSH) also acts as a substrate for Grxs, enzymes involved in the glutathionylation and deglutathionylation of cysteine sulfhydryl groups on various proteins (3, 13, 48). Much like thioredoxins, Grxs primarily maintain the cellular redox status. Grxs fall into two main groups:

The Buck Institute for Age Research, Novato, California.

dithiol Grxs including Grx1, which contains Cys-Pro-Tyr-Cys at the active site, and vertebrate Grx2, which contains a Cys-Ser-Tyr-Cys consensus sequence; and the monothiol Grxs, which contain Cys-Gly-Phe-Ser at the active site (including mitochondrial yeast Grx5 and vertebrate Grx1). Whereas mammalian dithiol Grx1 is reported to be localized exclusively in the cytosol within dopaminergic neurons (3), Grx2 is largely localized solely in the mitochondria, although a Grx2 isoform has been demonstrated to be targeted to the nucleus (19, 31, 32, 42). Grx1 and Grx2 have similar GSH-binding sites and hydrophobic surfaces; however, Grx2 also contains an Fe-S cluster that bridges two monomers of Grx2 and, as a result, acts as a redox sensor (29). Although these mammalian cytosolic and mitochondrial glutaredoxins share ~36% sequence identity, both Grx1 and Grx2 contain additional nonconserved cysteine residues outside of the active site that could contribute to differences in their inactivation and activation, respectively, during oxidative stress and may underlie various differences in function, depending on their subcellular localization (20). Monothiol Grx has been implicated in iron-sulfur center (Fe-S) biogenesis through control of proteins involved in the assembly (Grx5), as well as uptake of iron by regulation of the Aft1 transcription factor (Grx3/4; 21). In yeast, absence of *Grx5* results in reductions in respiratory growth and aberrant accumulation of iron within cells (38, 39). These alterations had been attributed to a reduction in Fe-S center synthesis and activity of enzymes containing such centers, including those involved in both mitochondrial function and cellular iron regulation.

Another recent study demonstrated that deficiency in the zebrafish homologue of yeast Grx5 also resulted in impaired Fe-S cluster assembly, suggesting that monothiol Grx homologues are involved in this process and, therefore, are evolutionarily conserved (49). Grx5 deficiency in zebrafish was found to result in conversion of cytosolic aconitase to its iron-regulatory protein 1 (IRP1) isoform, which normally acts to regulate cellular iron levels by controlling levels of the major iron-uptake protein transferrin and the iron-storage protein ferritin.

Grx2 is ubiquitously expressed throughout the brain, including within dopaminergic SN neurons. Previous studies showed that mammalian Grx2 effectively catalyzes the reversible glutathionylation/deglutathionylation of mitochondrial thiol proteins such as complex I (CI), which form mixed disulfides during oxidative conditions (7). Grx2 also functions as an essential component of the mitochondrial antioxidant defenses; selective knockdown of Grx2 levels by siRNA has been found to lead to increased sensitivity to oxidative stress–inducing apoptotic agents in HeLa cells (30). Recent studies also showed that selective knockdown of Grx2 by using antisense oligonucleotides results in partial loss of CI activity, suggesting that Grx2 is important in maintaining the function of this complex in mouse brain mitochondria (25).

In the present study, we assessed whether reduction in GSH as a substrate results in decreased Grx2 activity and, in turn, the possible impact of dithiol Grx2 inhibition on Fe-S center biogenesis and the enzymatic activity of Fe-S–containing enzymes involved in either mitochondrial function (CI, m-aconitase) or cellular iron homeostasis (cytosolic aconitase, IRP-1) within cultured dopaminergic cells. Our data for the first time suggest that GSH reduction and mammalian Grx2 inhibition through the impact on Fe-S center biogenesis result in disruptions in mitochondrial function and regulation of iron-regulatory proteins that control cellular iron levels.

Materials and Methods

Chemicals and reagents

All chemicals used in this study were obtained from Sigma (St. Louis, MO), unless otherwise noted. siRNA primers were designed and synthesized from Invitrogen (Carlsbad, CA). TRIzol reagent also was obtained from Invitrogen. DNA-free reagents were from Ambion (Austin, TX). TaqMan reverse-transcription reagent and SYBR Green PCR Master Mix were obtained from Applied Biosystems (Foster City, CA). All chemicals used were of at least analytic grade.

Tissue culture

All tissue-culture materials were procured from Cellgro (Kansas City, KS). For this study, we used N27 cells derived from embryonic rat dopaminergic mesencephalic neurons *via* SV40 large T antigen immortalization. These cells exhibit increased levels of tyrosine hydroxylase and dopamine transporter proteins and therefore consist of cells comparable to the midbrain dopaminergic neurons that are selectively lost in PD (1, 14). N27 cells were grown in RPMI medium 1640 containing 10% fetal bovine serum, penicillin (100 units/ml), and streptomycin (100 μg/ml). Glutathione was depleted by treatment of N27 cells with buthionine sulfoxamine (BSO) at a concentration of 0–40 μM for 0–72 h; previous studies demonstrated that 20 μM BSO results in a maximal 50% reduction in cellular glutathione, mimicking the depletion levels observed in the parkinsonian SN (11).

Mitochondrial preparations

Control, glutathione-depleted, or Grx2 siRNA–treated N27 cells were washed and resuspended in ice-cold isolation buffer (320 mM sucrose, 5 mM2-{[2-hydroxy-1,1-bis(hydroxymethyl) ethyl]amino}ethanesulfonic acid, and 1 mM EGTA, pH 7.4) followed by homogenization in a Dounce homogenizer. The homogenates were centrifuged at 1,000 g for 5 min at 4°C. Supernatant containing mitochondria was saved and pellet resuspended in isolation buffer and rehomogenized. Centrifugation of the resuspended homogenate was repeated, and the supernatants were pooled. The pooled supernatant was centrifuged at 10,000 g for 10 min at 4°C. The pellet containing the mitochondrion was resuspended in 50 μl isolation buffer for Grx2, mitochondrial CI, and m-aconitase enzyme activity assays. The purity of mitochondrial fractions for all subsequent studies was verified by assessing with Western blot with antibodies against the mitochondrial marker VDAC and the cytoplasmic actin.

Grx2 activity assay

Grx2 activity assay was performed as described by Gladyshev *et al.* (19), but with GSH provided endogenously (19). In brief, the reaction mixture contained 0.2 mM NADPH, 0.1 M potassium phosphate buffer (pH 7.4), 0.4 units of GSSG reductase, and 5 μg of mitochondrial fraction from control and treated samples in a total volume of 0.1 ml. After a 5-min preincubation with 2 mM synthetic substrate, hydroxyethyldisulfide (HEDS), the reaction was carried out at 30°C

for 5 min. The decrease in absorbance of NADPH at 340 nm was monitored by using the Spectra Max 340PC spectrophotometer (Molecular Devices, Sunnyvale, CA). To determine the Grx2 activity, the slope of the linear portion of the time course for 340-nm absorption loss in a control (Grx2-free) sample was subtracted from the slope of the samples containing Grx2.

Grx2 knockdown with siRNA

siRNA primers were designed by using the Invitrogen BLOCK-iT RNAi Designer tool. We purchased three sets of primers to determine those with the maximal knockdown efficiency of knockdown. The following oligonucleotides were designed, encoding the desired siRNA strands: target sequence 97 (TS-97) GGAAUGGGAAACAGCACAU (sense) and AUGUGCUGUUUCCCAUUCC (antisense); TS-206, CCUGCUCUUACUGUUCAAU (sense) and AUU GAACAGUAAGAGCAGG (antisense); and TS-396, GCUU CACAAAGAAGGGAAA (sense) and UUUCCCUUCUUUG UGAAGC (antisense). As a control, a nonspecific "scrambled" (scr) siRNA was designed by using the following oligonucleotides: scr, AACATTCACTCAGGTCATCAGCCTGTCTC (sense) and AACTGATGACCTG AGTGAATGCCTGTCTC (antisense). At 24 h before transfection, N27 cells were seeded in six-well plates, and transfection was performed at a cell confluence of 60% by using Lipofectamine 2000 (Invitrogen) according to the manufacturer's protocol. In brief, 20 n*M* 21-nt double-stranded siRNA in 50 μl of Opti-MEM I reduced serum and 12 μl of Lipofectamine 2000 in 50 μl of Opti-MEM I reduced serum were mixed and added to RPMI medium to yield a total volume of 2.0 ml. After 6 h of incubation, an equal volume of medium was added to the cells. The diluted transfection mix was removed after 24 h of transfection. The cells were washed twice with PBS before harvesting to perform RT-PCR to confirm the degree of Grx2 knockdown.

RT-PCR analysis of Grx2 and Grx1 mRNA

Total RNA was extracted from control and siRNA-transfected N27 cells by using Trizol (Invitrogen), and 2 μg was used to generate first-strand cDNA by using the SuperScript II reverse transcriptase kit (Invitrogen). Approximately 25 ng of cDNA was subject to PCR analysis by using the SYBR Green PCR Master Mix on the ABI prism 7900HT Sequence detection system (Applied Biosystems). Primers for Grx2, Grx1, actin, and GAPDH were designed based on nucleotide sequences found in Genbank. The PCR amplified products were run on a 2% agarose gel, and densitometry analysis was performed to evaluate the levels of Grx2 and Grx1 reduction by using actin or GAPDH as the internal control.

Dual Grx2 immunocytochemistry/Mitotracker red staining

N27 cells were seeded on glass plates to a density of 60% and transfected with siRNA primers (TS-396) for 24 h before fixation with 4% formaldehyde at room temperature for 30 min. Mitochondria were stained with 50 n*M* MitoTracker red (Molecular Probes) at 37°C for 30 min before fixation. Anti-Grx2 Ab (kindly provided by Dr. Lillig, Stockholm, Sweden) was preincubated for 2 h at room temperature at 1:10 dilution with 0.5 mg of BSA in 10 μl of PBS containing 0.3% Triton X-100. The Grx-2 antibody was then diluted 1:50 and incubated with the fixed cells in a moisture chamber at 4°C overnight. After washing with PBS 3×5 min, cells were incubated with the secondary Ab (1:250, Alexa Fluor 488 goat anti-rabbit IgG; Molecular Probes) for 60 min at room temperature. After 30-min washing with PBS, the slides were mounted and analyzed by using the fluorescence microscope Olympus BX51.

Immunoprecipitations of CI and m-aconitase

For immunoprecipitation of CI, mitochondria were isolated from control and BSO-treated N27 cells, as described earlier. Approximately 2 mg of mitochondria was washed with 20 m*M* Tris-HCl, pH 7.5, and 1 m*M* EDTA and suspended in the same buffer containing the protease inhibitor mixture. This suspension was solubilized by adding *n*-dodecyl-β-D-maltoside to a final concentration of 1% at 5 mg/ml protein concentration and incubated for 30 min on ice. Insoluble material from this suspension was removed by centrifugation at 55,000 *g* for 30 min at 4°C, and soluble material was taken for immunoprecipitation of CI by using the MS101 Complex I (CI) Immunocapture kit from MitoSciences (Eugene, OR) (43). In brief, the solubilized mitochondria was incubated with CI antibody linked with agarose beads for 3 h at RT or overnight at 4°C, followed by three quick washes with TE buffer containing protease inhibitors. Immunocaptured CI was then eluted with 10 μl of 0.1 *M* glycine, pH 2.5, supplemented with 0.05% *n*-dodecyl-β-D-maltoside. The eluted sample was then neutralized with 1 μl of 1 *M* Tris, pH 8.0. For immunoprecipitation of m-aconitase, ~1 mg of mitochondrial extract (in RIPA buffer containing anti-protease cocktail; Sigma) was incubated with aconitase antibody (#48915, kindly provided by Dr. Rick Eisenstein, University of Wisconsin-Madison) for at least 2 h to facilitate the formation of the antibody–antigen complex. This was followed by an overnight incubation with Red Protein A Affinity Gel and centrifugation to recover the immunoprecipitated mitochondrial aconitase bound to the beads. An aliquot of the antibody–antigen complex is mixed with sample buffer and boiled before running on an SDS-PAGE gel and stained with Sypro-Ruby (Bio-Rad) to determine its presence and abundance for normalization purposes.

ICP-MS assessment of iron incorporation

To determine the incorporation of iron into immunoprecipitated Fe-S cluster–containing enzymes, N27 cells were co-treated with 10 μM BSO and 50 μM Fe^{57} in normal RPMI medium for 72 h. Mitochondrial CI, m-aconitase, and cytosolic IRP-1 were immunoprecipitated, as earlier. Before analyses, immunoprecipitated samples were digested overnight with concentrated nitric acid, followed by a 20-min heating at 95°C, and redissolved in 1N Q-HNO_3. Total iron and Fe^{57} were measured by using a Varian Ultramass inductively coupled mass spectrometer (ICP-MS) under operating conditions suitable for routine multielement analysis (services were kindly provided by Irene Volitakis and Robert Cherny at The University of Melbourne Mental Health Research Institute, Australia).

Mitochondrial complex I assay

The mitochondrial CI enzyme assay was carried out as described by Trounce *et al.* (47). In brief, the assay was initiated

by addition of aliquots of mitochondria to 50 μM potassium phosphate, pH 7.4, 500 μM EDTA, 1% bovine serum albumin, 200 μM NADH, and 200 μM decylubiquinone with and without 2 μM rotenone in the presence of KCN, with 0.002% dichloroindophenol as a secondary electron acceptor. The decrease in the absorbance at 600 nm was recorded as a measure of enzyme reaction rate at 30°C for 10 min, and the specific activity was calculated. Values for all the assays were normalized per protein by using Bradford reagent (Bio-Rad, Hercules, CA).

Mitochondrial aconitase activity assay

From 5 to 10 μg of isolated mitochondrial extracts was incubated with a chemical cocktail of 30 mM sodium citrate, 0.6 mM $MnCl_2$, 0.2 mM $NADP^+$, and 2 units/ml of isocitrate dehydrogenase (in 25 mM KH_2PO_4 buffer). Readings were measured over a period of 5 min at 30°C (Abs = 340 nm), indicative of isocitrate formation with the release of NADPH.

IRP-binding assays

Cytoplasmic IRP-binding activities were assessed *via* an RNA gel-shift assay by using the I12CAT plasmid (gift of Dr. M.W. Hentze, EMBL, Heidelberg, Germany) that contains the IRE sequence of the human ferritin heavy chain under the control of T7 phage promoter. The plasmid is used to prepare the IRE RNA probe for the assay *via in vitro* transcription and ^{32}P labeling by using an RNA gel-shift kit from Fermentas, Inc. (Glen Burnie, MD) according to the manufacturer's instructions. Cellular homogenates (10 μg) were incubated with a molar excess of the ^{32}P-labeled IRE probe, as previously described. IRE-IRP1 complexes were then resolved on 6% non-denaturing acrylamide/bisacrylamide gels and quantified *via* autoradiography. β-Mercaptoethanol (β-ME) was added to aliquots of each sample as a control for loading.

TfR1 and ferritin Western blot analyses

Cells were homogenized in lysis buffer (0.15 M NaCl, 5 mM EDTA, pH 8, 1% Triton X100, 10 mM Tris-Cl, pH 7.4, DTT 50 mM) and centrifuged at 10,000 g. Protein concentration was determined in the supernatant by using Bradford reagent; 100 μg of protein per sample was mixed with sample buffer (100 mM Tris, pH 6.8, 2% SDS, 5% β-ME, 15% glycerol), boiled, and subjected to SDS-PAGE on a 4–12% gel. After transfer to PVDF membranes, the blots were probed with antibodies against TfR1 (Zymed, South San Francisco, CA; 1:1,000) and ferritin (Ramco, Stafford, TX; 1:500). TfR1 and ferritin levels were then detected by using HRP-conjugated secondary antibodies *via* ECL reagent (Amersham Biosciences, Piscataway, NJ). Actin was used as a loading control.

LIP measurements

The fluorescent probe calcein, which is quenched in the presence of iron (Fe^{3+}), was used to measure the labile iron pool (16). Cells were loaded with 25 mM calcein-AM for 30 min at room temperature, washed x3 with PBS to remove free dye, and counted. Calcein-loaded cells were then inoculated onto 96-well Optiplates (Perkin-Elmer Life Sciences, Boston, MA) at a density of 50,000 cells per well in 100 μl of PBS. Immediately before fluorescent measurements, SIH (cell-permeable iron chelator, kindly provided by Dr. P. Ponka, Montreal, Canada) was diluted in PBS, and 100 μl was added to the plates to give a final concentration of 100 μm for SIH. Triplicate wells were used for each condition. The plate was then read over timed intervals on a Molecular Devices fluorescent plate reader (488-nm excitation and 535-nm emission). For mitochondrial LIP measurement, the same method was slightly modified. The mitochondrial fraction was resuspended in PBS and loaded with calcein. After three washes, fractions of mitochondria corresponding to 5 μg protein were loaded per well. Fluorescent measurement at each time point for each treatment condition was averaged for the triplicate wells and graphed as a change in relative fluorescent units compared with untreated control cells or mitochondria.

Ferrozine assay

Total iron was measured with a modified ferrozine assay (34). Cytosolic or mitochondrial extracts were first incubated with concentrated hydrochloric acid to release iron from proteins, reduced with 75 mM ascorbate, and total iron levels were colorimetrically monitored (Abs = 562 nm) after the addition of 10 mM ferrozine and saturated ammonium acetate.

Statistical analyses

Values for all data were presented as mean ± SEM, and significance was assessed with a Student's t test. Differences were considered significant at $p < 0.05$. Data were collected from at least three cultures per condition in at least three separate experiments for all analyses.

Results

Glutathione depletion inhibits Grx2 activity in mammalian dopaminergic N27 cells in a dose-dependent manner

Previous studies showed that GSH acts a substrate for the Grx2 enzyme (17, 19). As GSH (and GSSG) depletion is the one of the earliest detectable biochemical alterations in PD and is known to affect both mitochondrial and iron regulatory functions involving Fe-S center-containing enzymes, we assessed the effect of GSH depletion on Grx2 activity in mitochondrial fractions isolated from our dopaminergic N27 cell line (Fig. 1A). The relative purity of mitochondrial fractions from experimental *versus* control cell populations for this and all subsequent studies was verified by assessing with Western blot by using antibodies against the mitochondrial marker VDAC and the cytoplasmic marker actin (Fig. 1B). N27 cells treated with increasing concentrations of BSO for 24 h displayed a concentration-dependent inhibition of Grx2 activity (Fig. 1; percentage of control 10 μM: 62.21 ± 8.3; 20 μM, 40.44 ± 7.21; 40 μM, 32.97 ± 3.3; $p < 0.05$; $n = 3$). This suggests that the GSH substrate is rate limiting for Grx2 activity in these cells.

siRNA-mediated knockdown of Grx2 in dopaminergic N27 cells

To monitor the role of GSH and Grx2 in iron incorporation into Fe-S center-containing enzymes and in their subsequent activities, we used an siRNA approach to knockdown Grx2 mRNA and protein levels in our N27 dopaminergic cell model. Of the three tested siRNA target sequences (siRNA-

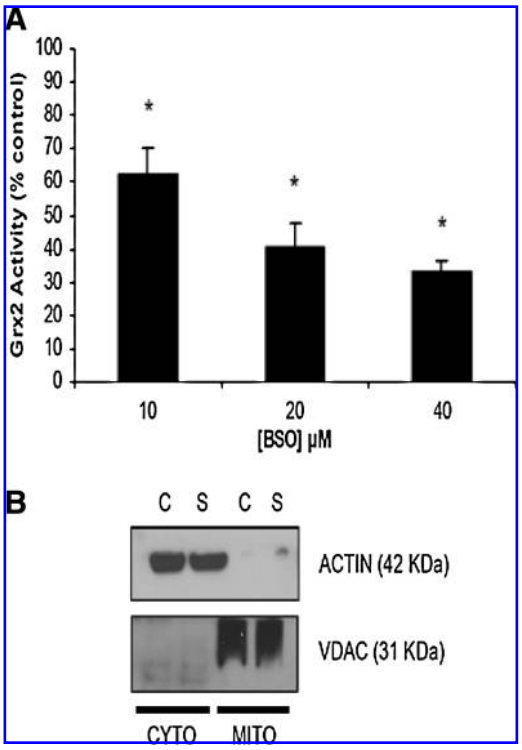

FIG. 1. Effect of total glutathione depletion on mitochondrial Grx2 activity in mammalian midbrain-derived dopaminergic N27 cells. (**A**) Measurement of Grx2 activity in mitochondrial fractions isolated from N27 cells treated with increasing concentrations of BSO for 24 h (0–40 μM). Activities are reported as percentage of control. $^*p < 0.05$, BSO treated compared with control. Experiments were repeated three times with $n = 3$. (**B**) Representative Western blot analyses verifying purity of mitochondrial fractions isolated from experimental *versus* control cell populations and used for assay of Grx2 enzyme activity and all subsequent experiments.

TS), two were found to be very effective in decreasing mRNA levels (97 and 396). Neither the transfection procedure itself nor the transfection of N27 cells with a control scrambled siRNA (siRNA-scr) had any effect on Grx2 mRNA levels (Fig. 2A) or subsequent protein or activity levels. Based on densitometry analysis of PCR products, siRNA-TS396 was found to be the most effective and was used for all subsequent experiments (data not shown).

We performed dual Grx2 immunocytochemistry and MitoTracker red staining to confirm a specific loss of Grx2 protein in the mitochondria on transfection of cells with siRNA-TS396. As shown in Fig. 2B, Grx2-specific staining in control cells colocalized well with MitoTracker red staining, indicating that Grx2 is located mainly in mitochondria of this dopaminergic cell line and that siRNA treatment effectively reduces Grx2 protein levels in this subcellular compartment. We further confirmed the loss of Grx2 mRNA and protein after siRNA transfection by measuring Grx2 activity. Two of the siRNA target sequences displayed more than an 80% inhibition of Grx2 activity compared with controls (Figs. 2C and 3A). Additionally, because Grx1 has recently been demonstrated to be localized within the mitochondrial intermembrane space in some cell types (35), RT-PCR analysis was performed to ensure that Grx1 was not affected by siRNA treatment with Grx2-specific primers (Fig. 2D).

Impact of glutathione depletion on iron incorporation into mitochondrial Fe-S center-containing enzymes and subsequent activity levels

We next assessed the impact of glutathione depletion on iron incorporation into Fe-S center-containing enzymes (*i.e.*, mitochondrial CI and m-aconitase) *via* ICP-MS analysis after their immunoprecipitation. Glutathione depletion by BSO significantly decreased the iron content in both mitochondrial CI and m-aconitase, as well as cytoplasmic aconitase (Fig. 3B and C; CI percentage of control, 54.55 ± 22.13; m-acon percentage of control, 50.52 ± 13.83; c-acon percentage of control, 89.46 ± 2.45; $p < 0.05$; $n = 3$). Grx2 silencing *via* siRNA in combination with GSH depletion did not enhance the reduction in iron levels (or subsequent Fe-S enzyme activities), suggesting that the two act in the same pathway (data not shown). Loss of iron incorporation into these enzymes may have contributed to significant decreases in their enzymatic activities, as reported in previous studies from our laboratory.

We did not study other Fe-S center containing mitochondrial complexes, as CI activity was selectively inhibited after GSH depletion (11, 22). We next determined whether Grx2 inhibition *via* siRNA would also affect mitochondrial function in our cellular model. We demonstrated an $\sim 60\%$ loss in m-aconitase (Fig. 4A; siRNA percentage of control, 58 ± 3.98; $p < 0.0001$; $n = 7$) and a nearly 30% loss in CI (Fig. 4B; siRNA percentage of control, 72.09 ± 11.27; $p < 0.05$; $n = 4$) activities compared with controls.

Impact of Grx2 siRNA on IRP1 binding, TfR and ferritin protein, and cellular iron levels

Unpublished data from our laboratory suggest that glutathione depletion has a significant impact on maintenance of iron homeostasis in dopaminergic cells (26). Therefore, to assess the impact of Grx2 inhibition as a consequence of glutathione depletion, we examined several aspects of iron regulation *in vitro*. Inhibition of Grx2 resulted in a 30% increase in IRP binding, presumably because of decreases in iron incorporation into Fe-S center-containing c-aconitase and resulting conversion to its non–Fe-S–containing IRP1 form (Figs. 3B and 4C). This was accompanied by increases in TfR and decreases in ferritin protein levels (Fig. 5). The labile iron pools (LIPs) within the cytosol and mitochondria (Fig. 6A) were measured, as well as total iron content, with the ferrozine assay (Fig. 6B; mitochondrial BSO-treated percentage of control 268.19; $p < 0.0001$; mitochondrial siRNA-treated percentage of control, 378.63 ± 86.8; $p < 0.05$; cytoplasmic BSO percentage of control, 135.42 ± 13.9; cytoplasmic siRNA-treated percentage of control, 133.6 ± 33.6; $n = 3$). Although no changes were observed in overall cytosolic iron levels, a significant increase in mitochondrial iron was noted after Grx inhibition.

Discussion

PD is characterized by depletions in SN glutathione (GSH and GSSG) levels early in the course of the disorder (4, 36, 37). Mitochondrial monothiol Grx5 that uses GSH as a substrate was recently demonstrated to be involved in the assembly of

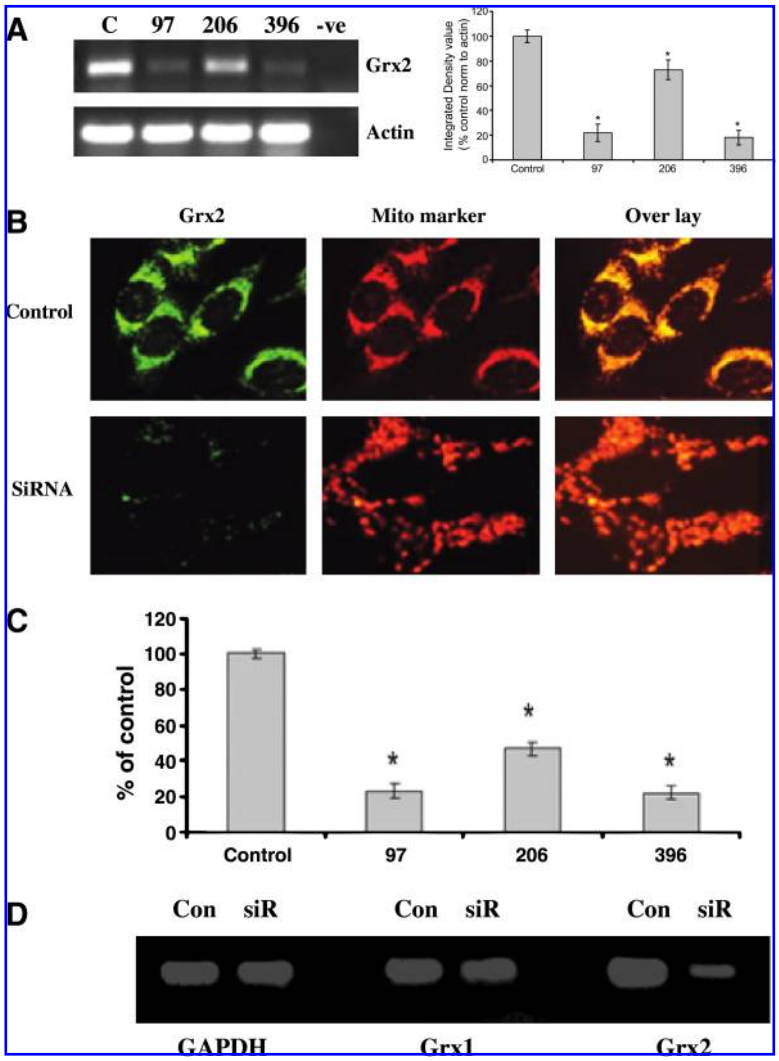

FIG. 2. siRNA-mediated knockdown of Grx2 in dopaminergic N27 cells. N27 cells transfected with three different primer sets (97, 206, 396) *via* Lipofectamine for 24 h. Control cells were transfected with scrambled siRNA (**C**) and mock transfected (-ve). (**A**) Representative RT-PCR analysis of Grx2 mRNA; actin RT-PCR was included as a control. (**B**) Representative dual Grx2 immunocytochemistry (Grx2) and mitotracker red staining (Mito marker) in cells transfected with 396 primer set (SiRNA) or scrambled (Control). (**C**) Grx2 activity after transfection with Grx2 siRNA primer sets 97, 206, and 396 *versus* scrambled control set in N27 cells. Activities are reported as percentage of control. (**D**) Representative RT-PCR analysis of Grx1 and Grx2 mRNA; GAPDH RT-PCR was included as a control. (For interpretation of the references to color in this figure legend, the reader is referred to the web version of this article at www.liebertonline.com/ars).

Fe-S centers in both yeast and zebrafish; these Fe-S centers are necessary for the activities of proteins involved in both mitochondrial function and cellular iron regulation, two processes strongly implicated in PD-related neurodegeneration. In contrast, in mammalian dopaminergic cells, the mitochondrial species of Grx is the dithiol enzyme Grx2 (28, 41). Although glutathione reduction in yeast does not appear to affect the activity of mitochondrial monothiol Grx5 (45), whether reductions in total dopaminergic glutathione levels affect mitochondrial function and cellular iron regulation *via* mitochondrial dithiol Grx2 and whether this involves effects on Fe-S center assembly have not yet been explored. Here we report that depletion of glutathione in dopaminergic cells results in enzymatic inhibition of Grx2 and subsequent decreases in iron incorporation into mitochondrial CI, m-aconitase, and cytosolic aconitase.

Grx2 inhibition also resulted in the inhibition of the enzymatic activities of CI and m-aconitase, which were accompanied by increases in mitochondrial iron levels. Elevations in IRP1 binding, increased transferrin receptor, and decreased ferritin protein levels also were observed. These data suggest that reduction in total dopaminergic glutathione levels can result in reduced dithiol Grx2 activity that may affect Fe-S center synthesis and in turn mitochondrial function and cellular iron homeostasis. In the Grx2 system, electrons are initially transferred from NADPH to glutathione reductase (GR), then to glutathione (GSH), and finally to Grx2. During chronic oxidative-stress conditions such as those that occur in the parkinsonian midbrain, GSH depletion can cause GR inhibition *via* a peroxynitrite-mediated mechanism (5). This can lead to further depletion of GSH levels and inhibition of Grx2 activity. Decreases in the NADPH pool can also dramatically reduce Grx2 activity.

Grx2 plays a major role in controlling redox signals and oxidative damage in the mitochondria by facilitating the interaction between the mitochondrial glutathione pool and protein thiols. Previous studies showed that Grx2 effectively catalyzes the reversible transient glutathionylation/deglutathionylation of mitochondrial thiol proteins, such as CI, that form mixed disulfides during oxidative conditions (7). However, during conditions of chronic oxidative stress, such as that observed in the parkinsonian midbrain, low levels of GSH and GSSG may inhibit Grx2 activity, preventing further transient protective mitochondrial protein glutathionylation, including at those cysteine residues found within Fe-S centers, ultimately leading to permanent damage *via* irreversible oxidation of those residues. This could prevent subsequent iron incorporation at Fe-S centers and inhibit the activity of

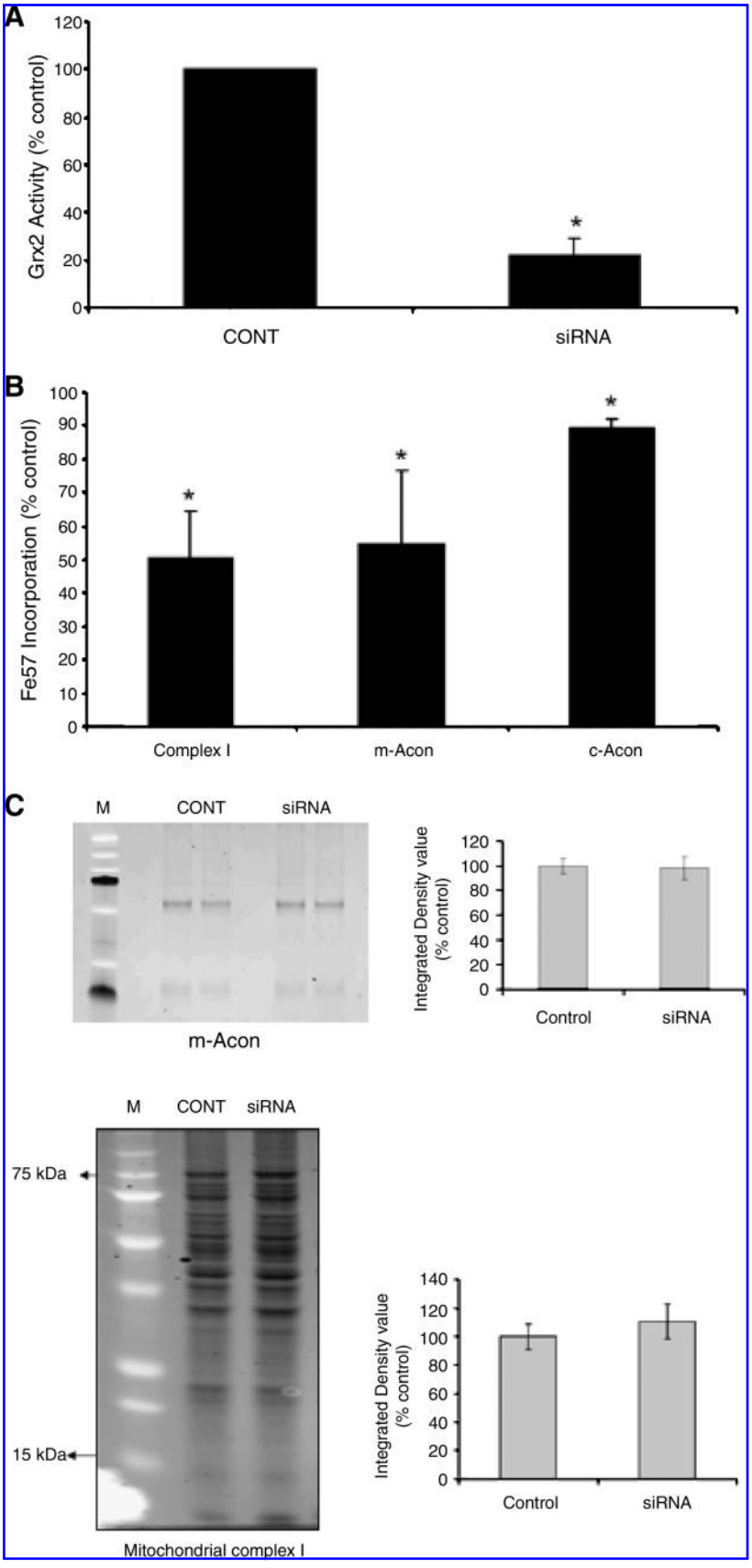

FIG. 3. Decreased Grx2 activity in N27 cells after siRNA transfection and reduced iron incorporation into mitochondria Fe-S–containing enzymes after GSH depletion. (**A**) Grx2 activity in N27 cells transfected with 396 primers for 24 h (CONT, mock transfected; siRNA, Grx2 396 siRNA-treated). Activities are reported as percentage of control. $*p < 0.0001$, siRNA treated compared with control ($n = 3$). (**B**) N27 cells treated with 10 μM BSO for 72 h, and mitochondria were harvested from these cells for immunoprecipitation of CI, m-aconitase, and c-aconitase for measurement of iron incorporation. ICP-MS analysis of ^{57}Fe levels in immunoprecipitated proteins; reported as percentage of control. $*p < 0.05$, BSO treated compared with control ($n = 3$). All experiments were repeated at least 3 times. (**C**) Representative examples of Sypro-Ruby gels verifying efficiency of IP of m-ACON (*upper panel*) and CI (*lower panel*) from control (CONT) and Grx2 siRNA-transfected (siRNA) cells. Molecular weight markers (M) are shown in lane 1.

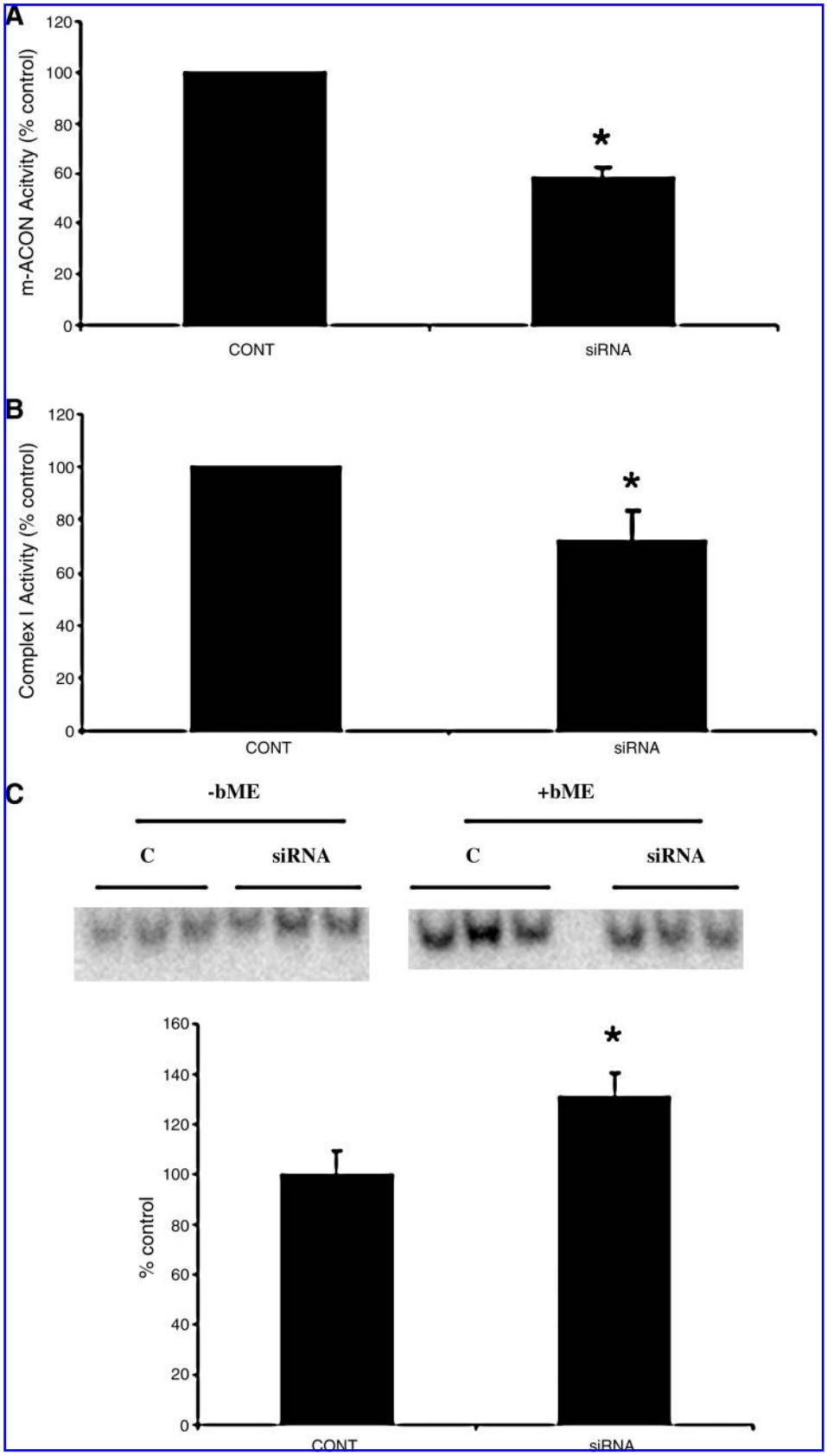

FIG. 4. Effect of Grx2 siRNA mitochondrial Fe-S center-containing enzyme activities. N27 cells were treated with siRNA TS-396 for 24 h before exchange with normal RPMI media for another 48 h before measurement of corresponding enzyme activities. (**A**) Mitochondrial aconitase (m-ACON) and (**B**) complex I. $^*p < 0.0001$ ($n = 7$) and $^*p < 0.05$ ($n = 4$), respectively, compared with control (CONT, mock-transfected; siRNA, 396 transfected, reported as percentage of control). (**C**) Representative IRP binding in mock transfected (C) or 396-transfected (siRNA); densitometric quantification was performed by using β-mercaptoethanol (+bME) as a normalizing control. Experiments were repeated 3 times with $n = 3$.

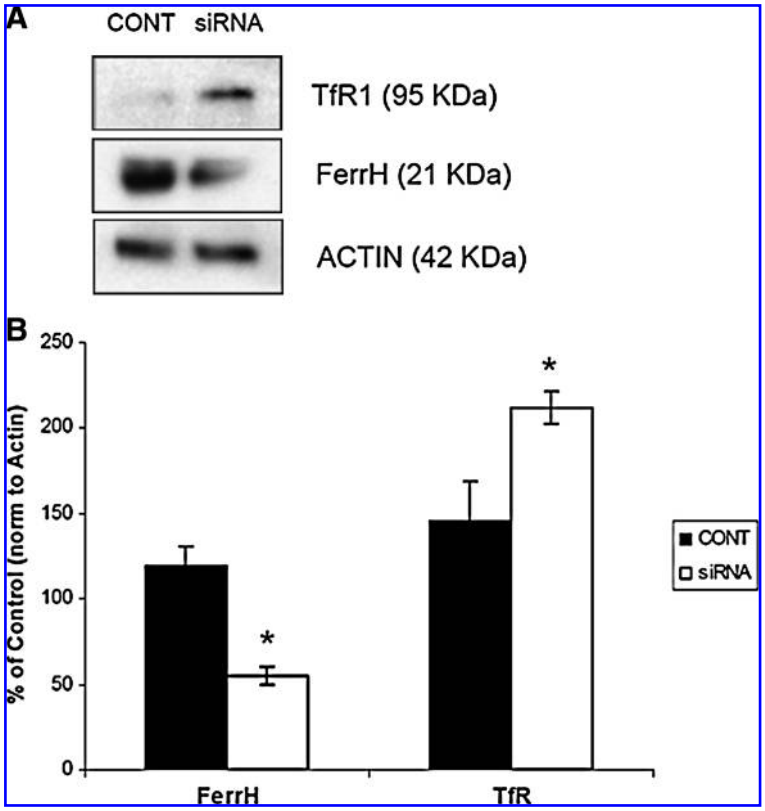

FIG. 5. Increased TFR1 and ferritin protein levels after Grx2 knockdown. (**A**) Representative Western blot analysis of TfR1 (TfR) and ferritin (FerrH) proteins from mock-transfected (CONT) controls *versus* 396-transfected (siRNA) cells. Actin is shown as loading control. (**B**) Band density (integrated density value) is expressed graphically as a percentage ratio of optical density of the TFR1 and ferritin proteins *versus* actin from three different Western blots. $*p < 0.05$, siRNA treated compared with controls.

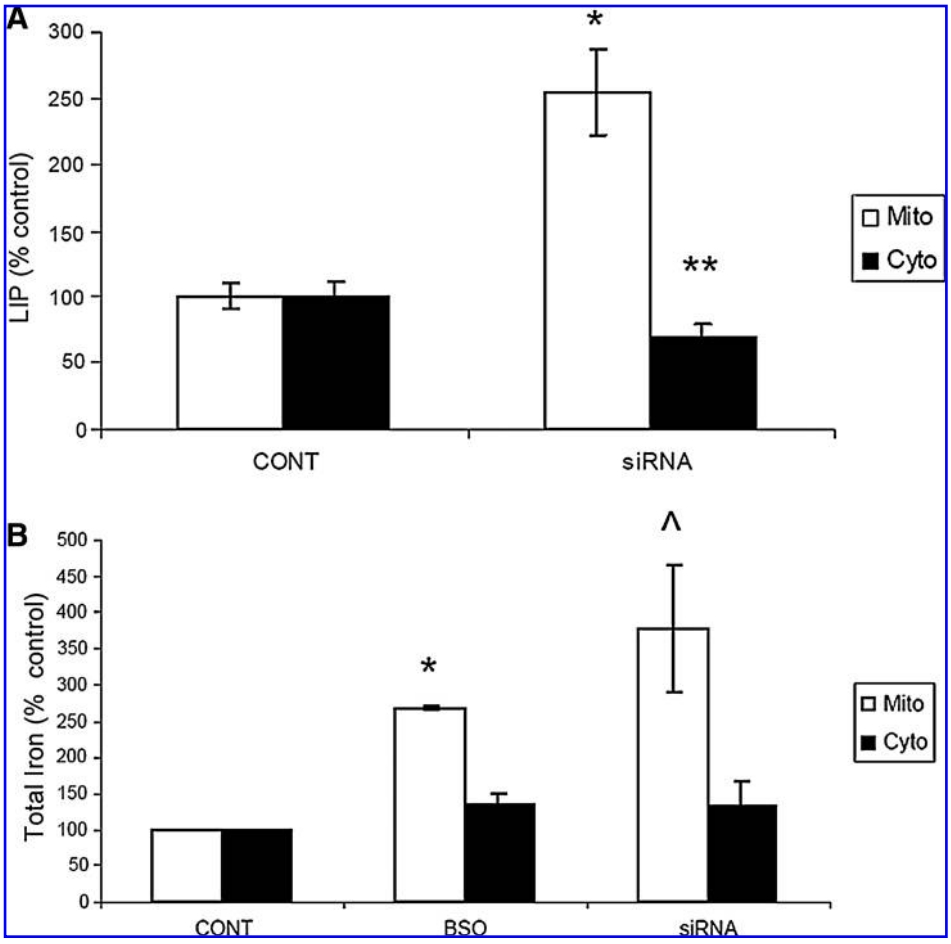

FIG. 6. Effect of Grx2 knockdown on labile iron pool content in N27 cells. (**A**) Mitochondrial (*white bars*) and cellular LIP levels were measured with Calcein dequenching after 5-min SIH treatment. $*p < 0.008$ siRNA treated compared with control. $**p < 0.05$ siRNA treated compared with control. Experiments were repeated three times with $n = 5$. (**B**) Mitochondrial (*white bars*) and cellular total iron content (*black bars*) as measured by ferrozine assay after mock-transfection (CONT), BSO, or 396 siRNA treatments. Experiments were repeated three times with $n = 3$.

Fe-S-center–containing enzymes involved in mitochondrial function and iron regulation. Insults that affect the iron-sulfur cluster biogenesis pathway have been suggested to be capable of influencing basic cellular processes and contributing to various human diseases (40). Grx2 knockdown *via* siRNA increases cellular sensitivity to oxidative stress–inducing apoptotic agents in HeLa cells (30), whereas its overexpression was found to decrease susceptibility of cells to apoptotic stimuli (15). Grx2 overexpression in Neuro2a cells was recently shown to abolish toxicity mediated by the parkinsonian neurotoxicant MPP^+ (25).

Grx2 itself is known to contain an Fe-S cluster, and spectroscopic analysis reveals a [2Fe-2S] cluster bridging two molecules of Grx2 (45). This Fe-S cluster is complexed by two N-terminal active-site thiols consisting of two Grx2 monomers and two molecules of GSH. The dimeric holo-Grx2 was enzymatically inactive, but it can be converted to its active monomeric form by oxidation of GSH to GSSG (29). In our dopaminergic PD model system, we believe that prolonged lack of both GSH and GSSG as substrates due to reductions in the total glutathione pool (emulating what occurs in the disease state itself) results in continued inhibition of Grx2, even in its active non–iron-binding form. It is also possible that the enzymatic activity of Grx2 is not the only factor resulting in the phenotypes observed after its depletion in midbrain dopaminergic cells but also loss of ability to bind to Fe-S centers (which interestingly requires the presence of GSH) (8). Alternatively, because the specific enzymatic activity of Grx1 is ~10-fold higher than that of Grx2 (33), it is possible that Grx1 may also contribute to the effects of mitochondrial Grx2 inhibition observed in this study. Although we were not able to demonstrate the absence of Grx1 in our mitochondrial preparations because of technical issues, we did not observe any changes in its mRNA levels after knockdown of Grx2 (Fig. 2D).

PD is characterized by both mitochondrial dysfunction and iron dysregulation. Our data suggest that these effects involve glutathione depletion–mediated Grx2 inhibition and its effects on mitochondrial Fe-S biogenesis. The phenotype we observe after Grx2 inhibition remarkably resembles phenotypes resulting from the silencing of other proteins involved in Fe-S cluster assembly in mammalian cells, including frataxin (45) and Nfs1 (9).

It is not clear mechanistically what causes the observed increase in mitochondrial iron levels and decrease in cytosolic iron, but it is likely a compensatory action by the cell in an aberrant attempt to enhance mitochondrial Fe-S assembly by increasing mitochondrial iron levels. The increase in mitochondrial iron levels fits with previous reports of this occurrence as a consequence of disruption of mitochondrial Fe-S assembly (27, 44). This may involve compensatory increases in mitochondrial iron import or stability as a consequence of, for example, TfR2 increase or frataxin reduction as a consequence of GSH reduction (2). We are currently exploring these possibilities in our model system.

Acknowledgments

This work was supported by National Institutes of Health grants R01 NS041264, R01 NS045615, and PPG AG025901 (J.K.A.), and D.W.L. is a recipient of a postdoctoral fellowship from the Larry L. Hillblom foundation.

Author Disclosure Statement

No competing financial interests exist.

References

1. Adams FS, La Rosa FG, Kumar S, Edwards-Prasad J, Kentroti S, Vernadakis A, Freed CR, and Prasad KN. Characterization and transplantation of two neuronal cell lines with dopaminergic properties. *Neurochem Res* 21: 619–627, 1996.
2. Auchere F, Santos R, Planamente S, Lesuisse E, and Camadro JM. Glutathione-dependent redox status of frataxin-deficient cells in a yeast model of Friedreich's ataxia. *Hum Mol Genet* 17: 2790–2802, 2008.
3. Balijepalli S, Tirumalai PS, Swamy K, Boyd V, Mieyal MR, Ravindranath JJ, and Rat V. Brain thioltransferase: regional distribution, immunological characterization, and localization by fluorescent in situ hybridization. *J Neurochem* 72: 1170–1178, 1999.
4. Bannon MJ, Goedert M, and Williams B. The possible relation of glutathione, melanin and 1-methyl-4-phenyl-1,2,5,6-tetrahydropyridine (MPTP) to Parkinson's disease. *Biochem Pharmacol* 33: 2697–2698, 1984.
5. Barker JE, Heales SJ, Cassidy A, Bolanos JP, Land J, Clark M, and Jones B. Depletion of brain glutathione results in a decrease of glutathione reductase activity; an enzyme susceptible to oxidative damage. *Brain Res* 716: 118–122, 1996.
6. Beal MF. Does impairment of energy metabolism result in excitotoxic neuronal death in neurodegenerative illnesses? *Ann Neurol* 31: 119–130, 1992.
7. Beer SM, Taylor ER, Brown SE, Dahm CC, Costa NJ, Runswick MJ, and Murphy MP. Glutaredoxin 2 catalyzes the reversible oxidation and glutathionylation of mitochondrial membrane thiol proteins: implications for mitochondrial redox regulation and antioxidant defense. *J Biol Chem* 279: 47939–47951, 2004.
8. Berndt C, Hudemann C, Hanschmann EM, Axelsson R, Holmgren A, and Lillig CH. How does iron-sulfur cluster coordination regulate the activity of human glutaredoxin 2? *Antioxid Redox Signal* 9: 151–157, 2007.
9. Biederbick A, Stehling O, Rosser R, Niggemeyer B, Nakai Y, Elsasser HP, and Lill R. Role of human mitochondrial Nfs1 in cytosolic iron-sulfur protein biogenesis and iron regulation. *Mol Cell Biol* 26: 5675–5687, 2006.
10. Burke RE. Programmed cell death and Parkinson's disease. *Mov Disord* 13(suppl 1): 17–23, 1998.
11. Chinta SJ and Andersen RK. Reversible inhibition of mitochondrial complex I activity following chronic dopaminergic glutathione depletion in vitro: implications for Parkinson's disease. *Free Radic Biol Med* 41: 1442–1448, 2006.
12. Chinta SJ, Kumar MJ, Hsu M, Rajagopalan S, Kaur D, Rane A, Nicholls DG, Choi J, and Andersen JK. Inducible alterations of glutathione levels in adult dopaminergic midbrain neurons result in nigrostriatal degeneration. *J Neurosci* 27: 13997–14006, 2007.
13. Cohen G and Kesler N. Monoamine oxidase and mitochondrial respiration. *J Neurochem* 73: 2310–2315, 1999.
14. Clarkson ED, Rosa FG, Edwards-Prasad J, Weiland DA, Witta SE, Freed CR, and Prasad KN. Improvement of neurological deficits in 6-hydroxydopamine-lesioned rats after transplantation with allogeneic simian virus 40 large tumor antigen gene-induced immortalized dopamine cells. *Proc Natl Acad Sci U S A* 95: 1265–1270, 1998.
15. Enoksson M, Fernandes AP, Prast S, Lillig CH, Holmgren A, and Orrenius S. Overexpression of glutaredoxin 2 attenuates

apoptosis by preventing cytochrome c release. *Biochem Biophys Res Commun* 327: 774–779, 2005.
16. Epsztejn S, Kakhlon O, Glickstein H, Breuer W, and Cabantchik I. Fluorescence analysis of the labile iron pool of mammalian cells. *Anal Biochem* 248: 31–40, 1997.
17. Fernando MR, Lechner JM, Lofgren S, Gladyshev VN, and Lou MF. Mitochondrial thioltransferase (glutaredoxin 2) has GSH-dependent and thioredoxin reductase-dependent peroxidase activities in vitro and in lens epithelial cells. *FASEB J* 20: 2645–2647, 2006.
18. Forno LS. Neuropathology of Parkinson's disease. *J Neuropathol Exp Neurol* 55: 259–272, 1996.
19. Gladyshev VN, Liu A, Novoselov A, Krysan SV, Sun K, Kryukov QA, Kryukov VM, Lou GV, and M F. Identification and characterization of a new mammalian glutaredoxin (thioltransferase), Grx2. *J Biol Chem* 276: 30374–30380, 2001.
20. Hashemy SI, Johansson C, Berndt C, Lillig CH, and Holmgren A. Oxidation and s-nitrosylation of cysteines in human and mitochondrial glutaredoxins. *J Biol Chem* 282: 14428–14436, 2007.
21. Herrero E and de la Torre-Ruiz MA. Monothiol glutaredoxins: a common domain for multiple functions. *Cell Mol Life Sci* 64: 1518–1530, 2007.
22. Hsu M, Srinivas B, Kumar J, Subramanian R, and Andersen J. Glutathione depletion resulting in selective mitochondrial complex I inhibition in dopaminergic cells is via an NO-mediated pathway not involving peroxynitrite: implications for Parkinson's disease. *J Neurochem* 92: 1091–1103, 2005.
23. Jenner P. Altered mitochondrial function, iron metabolism and glutathione levels in Parkinson's disease. *Acta Neurol Scand Suppl* 146: 6–13, 1993.
24. Jha N, Jurma O, Lalli O, Liu G, Pettus Y, Greenamyre EH, Liu JT, Forman RM, Andersen HJ, and Andersen JK. Glutathione depletion in PC12 results in selective inhibition of mitochondrial complex I activity: implications for Parkinson's disease. *J Biol Chem* 275: 26096–26101, 2000.
25. Karunakaran S, Saeed U, Ramakrishnan S, Koumar RC, and Ravindranath V. Constitutive expression and functional characterization of mitochondrial glutaredoxin (Grx2) in mouse and human brain. *Brain Res* 1185: 817, 2007.
26. Kaur D, Lee DW, Rajagopalan S, and Andersen JK. Glutathione depletion in immortalized midbrain-derived dopaminergic neurons results in increases in the labile iron pool: implications for Parkinson's disease. *Free Radic Biol Med* 46: 593–598, 2009.
27. Li K, Besse EK, Ha D, Kovtunovych G, and Rouault TA. Iron-dependent regulation of frataxin expression: implications for treatment of Friedreich ataxia. *Hum Mol Genet* 17: 2265–2273, 2008.
28. Lillig CH, Berndt C, and Holmgren A. Glutaredoxin systems. *Biochim Biophys Acta* 1780: 1304–1317, 2008.
29. Lillig CH, Berndt C, Vergnolle O, Lonn ME, Hudemann C, Bill E, and Holmgren A. Characterization of human glutaredoxin 2 as iron-sulfur protein: a possible role as redox sensor. *Proc Natl Acad Sci U S A* 102: 8168–8173, 2005.
30. Lillig CH, Lonn ME, Enoksson M, Fernandes AP, and Holmgren A. Short interfering RNA-mediated silencing of glutaredoxin 2 increases the sensitivity of HeLa cells toward doxorubicin and phenylarsine oxide. *Proc Natl Acad Sci U S A* 101: 13227–13232, 2004.
31. Lundberg M, Fernandes AP, Kumar S, and Holmgren A. Cellular and plasma levels of human glutaredoxin 1 and 2 detected by sensitive ELISA systems. *Biochem Biophys Res Commun* 319: 801–809, 2004.
32. Lundberg M, Johansson C, Chandra C, Enoksson J, Jacobsson M, Ljung G, Johansson J, and Holmgren MA. Cloning and expression of a novel human glutaredoxin (Grx2) with mitochondrial and nuclear isoforms. *J Biol Chem* 276): 26269–26275, 2001.
33. Missirlis F, Holmberg S, Georgieva T, Dunkov BC, Rouault TA, and Law JH. Characterization of mitochondrial ferritin in *Drosophila. Proc Natl Acad Sci U S A* 103: 5893–5898, 2006.
34. Mieyal JJ, Gallogly MM, Qanungo S, Sabens EA, and Shelton MD. Molecular mechanisms and clinical implications of reversible protein S-glutathionylation. *Antioxid Redox Signal* 10: 1941–1988, 2008.
35. Pai HV, Starke DW, Lesnefsky EJ, Hoppel CL, and Mieyal JJ. What is the functional significance of the unique location of glutaredoxin 1 (GRx1) in the intermembrane space of mitochondria? *Antioxid Redox Signal* 9: 2027–2033, 2007.
36. Perry TL, Godin DV, Hansen S. Parkinson's disease: a disorder due to nigral glutathione deficiency? *Neurosci Lett* 33: 305–310, 1982.
37. Perry TL and Yong VW. Idiopathic Parkinson's disease, progressive supranuclear palsy and glutathione metabolism in the substantia nigra of patients. *Neurosci Lett* 67: 269–274, 1986.
38. Rodriguez-Manzaneque MT, Ros J, Cabiscol E, Sorribas A, and Herrero E. Grx5 glutaredoxin plays a central role in protection against protein oxidative damage in *Saccharomyces cerevisiae. Mol Cell Biol* 19: 8180–8190, 1999.
39. Rodriguez-Manzaneque MT, Tamarit J, Belli G, Ros J, and Herrero E. Grx5 is a mitochondrial glutaredoxin required for the activity of iron/sulfur enzymes. *Mol Biol Cell* 13: 1109–1121, 2002.
40. Rouault TA and Tong WH. Iron-sulfur cluster biogenesis and human disease. *Trends Genet* 24: 398–407, 2008.
41. Sagemark J, Elgan TH, Burglin TR, Johansson C, Holmgren A, and Berndt KD. Redox properties and evolution of human glutaredoxins. *Proteins* 68: 879–892, 2007.
42. Saeed U, Durgadoss L, Valli RK, Joshi DC, Joshi PG, and Ravindranath V. Knockdown of cytosolic glutaredoxin 1 leads to loss of mitochondrial membrane potential: implications in neurodegenerative diseases. *PLoS ONE* 3: e2459, 2008.
43. Schilling B, Bharath MM, Row RH, Murray J, Cusack MP, Capaldi RA, Freed CR, Prasad KN, Andersen JK, and Gibson BW. Rapid purification and mass spectrometric characterization of mitochondrial NADH dehydrogenase (Complex I) from rodent brain and a dopaminergic neuronal cell line. *Mol Cell Proteomics* 4: 84–96, 2005.
44. Schueck ND, Woontner M, and Koeller DM. The role of the mitochondrion in cellular iron homeostasis. *Mitochondrion* 1: 51–56, 2001.
45. Sipos K, Lange H, Fekete Z, Ullmann P, Lill R, and Kispal G. Maturation of cytosolic iron-sulfur proteins requires glutathione. *J Biol Chem* 277: 26944–26949, 2002.
46. Stehling O, Elsasser HP, Bruckel B, Muhlenhoff U, and Lill R. Iron-sulfur protein maturation in human cells: evidence for a function of frataxin. *Hum Mol Genet* 13: 3007–3015, 2004.
47. Trounce IA, Kim YL, Jun AS, and Wallace DC. Assessment of mitochondrial oxidative phosphorylation in patient muscle biopsies, lymphoblasts, and transmitochondrial cell lines. *Methods Enzymol* 264: 484–509, 1996.
48. Wang J, Boja ES, Tan W, Tekle E, Fales HM, English S, Mieyal JJ, and Chock P. B. Reversible glutathionylation regulates actin polymerization in A431 cells. *J Biol Chem* 276: 47763–47766, 2001.

49. Wingert RA, Galloway JL, Barut B, Foott H, Fraenkel P, Axe JL, Weber GJ, Dooley K, Davidson AJ, Schmid B, Paw BH, Shaw GC, Kingsley P, Palis J, Schubert H, Chen O, Kaplan J, and Zon LI. Deficiency of glutaredoxin 5 reveals Fe-S clusters are required for vertebrate haem synthesis. *Nature* 436: 1035–1039, 2005.

Address correspondence to:
Julie K. Andersen, Ph.D.
Buck Institute for Age Research
8001 Redwood Blvd
Novato, CA 94945

E-mail: jandersen@buckinstitute.org

Date for first submission to ARS Central, January 27, 2009; date of final revised submission, March 10, 2009; date of acceptance, March 14, 2009.

Abbreviations Used

ACON = aconitase
CI = mitochondrial complex I
Fe-S cluster = iron-sulfur cluster
Grx2 = glutaredoxin 2
GSH = glutathione
IRP = iron regulatory protein
LIP = labile iron pool
PD = Parkinson's disease
TfR1 = transferritin receptor

This article has been cited by:

1. Humberto Rodriguez-Rocha , Aracely Garcia Garcia , Laura Zavala-Flores , Sumin Li , Nandakumar Madayiputhiya , Rodrigo Franco . Glutaredoxin 1 Protects Dopaminergic Cells by Increased Protein Glutathionylation in Experimental Parkinson's Disease. *Antioxidants & Redox Signaling*, ahead of print. [Abstract] [Full Text HTML] [Full Text PDF] [Full Text PDF with Links] [Supplemental material]
2. Lei Wang, Bingjie Ouyang, Yifei Li, Yingang Feng, Jean-Pierre Jacquot, Nicolas Rouhier, Bin Xia. 2012. Glutathione regulates the transfer of iron-sulfur cluster from monothiol and dithiol glutaredoxins to apo ferredoxin. *Protein & Cell* **3**:9, 714-721. [CrossRef]
3. Fei Yin , Harsh Sancheti , Enrique Cadenas . Mitochondrial Thiols in the Regulation of Cell Death Pathways. *Antioxidants & Redox Signaling*, ahead of print. [Abstract] [Full Text HTML] [Full Text PDF] [Full Text PDF with Links]
4. Aracely Garcia-Garcia , Laura Zavala-Flores , Humberto Rodriguez-Rocha , Rodrigo Franco . Thiol-Redox Signaling, Dopaminergic Cell Death, and Parkinson's Disease. *Antioxidants & Redox Signaling*, ahead of print. [Abstract] [Full Text HTML] [Full Text PDF] [Full Text PDF with Links]
5. Seila Fernandez#Fernandez, Angeles Almeida, Juan P. Bolaños. 2012. Antioxidant and bioenergetic coupling between neurons and astrocytes. *Biochemical Journal* **443**:1, 3-11. [CrossRef]
6. Elizabeth A. Sabens Liedhegner , Xing-Huang Gao , John J. Mieyal . 2012. Mechanisms of Altered Redox Regulation in Neurodegenerative Diseases—Focus on S-Glutathionylation. *Antioxidants & Redox Signaling* **16**:6, 543-566. [Abstract] [Full Text HTML] [Full Text PDF] [Full Text PDF with Links]
7. L. Brautigam, L. D. Schutte, J. R. Godoy, T. Prozorovski, M. Gellert, G. Hauptmann, A. Holmgren, C. H. Lillig, C. Berndt. 2011. Vertebrate-specific glutaredoxin is essential for brain development. *Proceedings of the National Academy of Sciences* . [CrossRef]
8. Garima Srivastava, Anubhuti Dixit, Om Prakash, Mahendra Pratap Singh. 2011. Tiny non-coding RNAs in Parkinson's disease: Implications, expectations and hypes. *Neurochemistry International* **59**:6, 759-769. [CrossRef]
9. Bastian Hoffmann , Marta A. Uzarska , Carsten Berndt , José R. Godoy , Petra Haunhorst , Christopher Horst Lillig , Roland Lill , Ulrich Mühlenhoff . 2011. The Multidomain Thioredoxin-Monothiol Glutaredoxins Represent a Distinct Functional Group. *Antioxidants & Redox Signaling* **15**:1, 19-30. [Abstract] [Full Text HTML] [Full Text PDF] [Full Text PDF with Links] [Supplemental material]
10. Xiang Ming Xu , Simon Geir Møller . 2011. Iron–Sulfur Clusters: Biogenesis, Molecular Mechanisms, and Their Functional Significance. *Antioxidants & Redox Signaling* **15**:1, 271-307. [Abstract] [Full Text HTML] [Full Text PDF] [Full Text PDF with Links]
11. Natalia P. Mena, Anne Laure Bulteau, Julio Salazar, Etienne C. Hirsch, Marco T. Núñez. 2011. Effect of mitochondrial complex I inhibition on Fe–S cluster protein activity. *Biochemical and Biophysical Research Communications* **409**:2, 241-246. [CrossRef]
12. Chitranshu Kumar, Aeid Igbaria, Benoît D'Autreaux, Anne-Gaëlle Planson, Christophe Junot, Emmanuel Godat, Anand K Bachhawat, Agnès Delaunay-Moisan, Michel B Toledano. 2011. Glutathione revisited: a vital function in iron metabolism and ancillary role in thiol-redox control. *The EMBO Journal* **30**:10, 2044-2056. [CrossRef]
13. Gabriele Gille, Heinz Reichmann. 2011. Iron-dependent functions of mitochondria—relation to neurodegeneration. *Journal of Neural Transmission* **118**:3, 349-359. [CrossRef]
14. A. Ferri, P. Fiorenzo, M. Nencini, M. Cozzolino, M. G. Pesaresi, C. Valle, S. Sepe, S. Moreno, M. T. Carri. 2010. Glutaredoxin 2 prevents aggregation of mutant SOD1 in mitochondria and abolishes its toxicity. *Human Molecular Genetics* **19**:22, 4529-4542. [CrossRef]
15. Jakob Nyhlén, Radu Constantinescu, Henrik Zetterberg. 2010. Problems associated with fluid biomarkers for Parkinson's disease. *Biomarkers in Medicine* **4**:5, 671-681. [CrossRef]
16. Nicolas Rouhier, Jérémy Couturier, Michael K. Johnson, Jean-Pierre Jacquot. 2010. Glutaredoxins: roles in iron homeostasis. *Trends in Biochemical Sciences* **35**:1, 43-52. [CrossRef]
17. Kevin G. Hoff, Stephanie J. Culler, Peter Q. Nguyen, Ryan M. McGuire, Jonathan J. Silberg, Christina D. Smolke. 2009. In Vivo Fluorescent Detection of Fe-S Clusters Coordinated by Human GRX2. *Chemistry & Biology* **16**:12, 1299-1308. [CrossRef]
18. Bobby Thomas . 2009. Parkinson's Disease: From Molecular Pathways in Disease to Therapeutic Approaches. *Antioxidants & Redox Signaling* **11**:9, 2077-2082. [Abstract] [Full Text HTML] [Full Text PDF] [Full Text PDF with Links]